Visual Abstract

Impact behaviour of dissimilar AA2024-T351/7075-T651 FSWed butt-joints: effects of Al_2O_3-SiC particles addition

Cindy Morales, Mattia Merlin, Annalisa Fortini, Gian Luca Garagnani
Department of Engineering, University of Ferrara, Via Saragat 1, 44122 Ferrara, Italy
mrlcdy@unife.it, http://orcid.org/0000-0001-8536-1742
mattia.merlin@unife.it, http://orcid.org/0000-0003-4685-1073
annalisa.fortini@unife.it, http://orcid.org/0000-0002-9774-7105
gian.luca.garagnani@unife.it, http://orcid.org/0000-0002-5403-0868

Argelia Miranda
Universidad Popular Autónoma del Estado de Puebla, 17 Sur, 901, Barrio de Santiago, 72410, Puebla, México
argeliafabiola.miranda@upaep.mx, http://orcid.org/0000-0002-6168-0279

ABSTRACT. Dissimilar friction stir welding joints are widely employed in the industrial field due to the excellent microstructural and mechanical properties of the resulting joints. Nevertheless, to further enhance the weld properties, the addition of reinforcement particles on the joint-line during the process has been proven effective for increasing its mechanical performance. In the present investigation, the microstructure and the impact behaviour of FSWed joints between AA2024-T351 and AA7075-T651 aluminium plates were investigated, considering the effect of different process parameters selected through a full factorial 2^k design of experiments: both the rotational and translational speed of the tool, as well as the addition of Al_2O_3-SiC microparticles, were considered as input parameters. Unnotched 10 x 5 x 55 mm impact specimens were tested through an instrumented 50 J Charpy pendulum: total impact energy, the two complementary initiation and propagation energies as well as the peak force were correlated to the adopted process parameters. From the performed analyses, it was found that joints with reinforcing particles are prone to form wormhole defects across the stir zone that not only affect the microstructural development, but also the impact behaviour since they require less energy at break in comparison with joints fabricated without particles addition.

KEYWORDS. Friction stir welding; Impact strength; Dissimilar joints; Particles-reinforcement; Microstructure.

OPEN ACCESS

Citation: Morales, C., Merlin, M., Fortini, A., Garagnani, G.L., Miranda A. Impact behavior of dissimilar AA2024-T351/7075-T651 FSWed butt-joints: effects of Al2O3-SiC particles addition, Frattura ed Integrità Strutturale, 60 (2022) 505-515.

Received: 28.02.2022
Accepted: 23.03.2022
Online first: 24.02.2022
Published: 01.04.2022

Copyright: © 2022 This is an open access article under the terms of the CC-BY 4.0, which permits unrestricted use, distribution, and reproduction in any medium, provided the original author and source are credited.

INTRODUCTION

Friction Stir Welding (FSW), as a solid-state bonding procedure, is one of the most commonly used techniques to join different materials able to guarantee suitable microstructural and mechanical characteristics, highly competitive in industrial sectors such as automotive and aerospace [1–4]. The employment of FSW procedure has been increasing through the years and its development has promoted innovations in terms of equipment and research studies. Dissimilar joints are one of these kinds of innovative weld arrangements intended to increase specific mechanical features of a component with the union of the features of two different alloys. Nevertheless, high-quality welds are the result of comprehensive control of the process due to the different features of the different materials, which could lead to inadequate heat generation and material flow, thus affecting the mechanical and microstructural behaviour of the final joint [5–9]. Recently, not only the use of different alloys, but also the introduction of particles across the joint line during the welding procedure, has gained attention since a remarkable increase of the mechanical features of the joint can be achieved.

In literature, the static properties of similar FSWed aluminium alloys have been deeply investigated and several studies focused on the effect that the addition of reinforcing particles has on the mechanical properties of FSWed joints. Salehi et al. [10] added SiC nanoparticles into the groove of an AA6061 joint before the friction stir processing, finding that the volume fraction of the nano-SiC particles has an important effect on the final mechanical properties of the joint with respect to samples obtained without any kind of reinforcement. More recently, Balaji et al. [11] demonstrated that samples of FSW AA6063 similar joints produced with the addition of B_4C powder show higher hardness and impact properties than the un-reinforced ones, while the tensile behaviour worsens when the reinforcement is present. Similarly, Kumar et al. [12] investigated the effect of reinforcing particles addition into an AA6061 alloy, finding that the size and type of the particles significantly influence and, in most cases, enhance the hardness and wear behaviour of the joint while decreasing its tensile properties. Nevertheless, most researchers agree that adding reinforcing particles in similar aluminium joints improve the static mechanical properties.

In latest years, different researchers focused their studies on the production of reinforced aluminium dissimilar alloys. Muhamad et al. [13] produced dissimilar AA7075-AISI304 FSW-joints investigating the effect of the addition of a different amount of Al-Ni powder into the joint-line. The authors detected a metallurgical reaction as an effect of the reinforcing addition, thus promoting an increase of the tensile properties of the joint; however, they found that the selection of specific process parameters, in this case low rotational speed, is fundamental to obtain the desired increase in the static mechanical characteristics. Recently, Vimalraj et al. [14] performed a review on the advantages and disadvantages of the use of reinforcing particles into the groove of dissimilar joints during the process; they emphasize the remarkable effect induced by the process parameters on the particles dispersion and, in turn, on the mechanical properties of the joints. Moreover, the authors pointed out that more studies need to be done in terms of comparison of different dissimilar joints production and on the optimization of amount, type and size of the reinforcement together with the number of welding passes.

The Charpy impact test is another very useful and straightforward experimental method to assess the effect of process parameters and microstructure on the impact strength of metallic materials [15] and, in particular, of aluminium alloys [16–22]. To the author's knowledge, to date the impact behaviour of similar and dissimilar FSWed aluminium alloys has not been deeply studied [12,16,23,24]. In the automotive/aerospace field, the need for high resistant and low-density joints is very strictly; to this objective, dissimilar AA2024-AA7075 joints have been deeply investigated [25–27] but no data are available in literature as concern impact strength and the influence of reinforcing particles in the absorbed energy.

The aim of the present work is to study the influence of the addition of Al_2O_3-SiC reinforcing particles on the impact properties of FSWed AA2024-AA7075 dissimilar joints. The joints were produced with different process parameters selected according to a full factorial 2^k design of experiments. The microstructural features induced by the different process parameters were correlated to the experimental findings in terms of total absorbed energy, initiation and propagation energies as well as the peak force of un-notched Charpy samples drawn from the joints. Furthermore, microstructural and fractographic analyses were performed to investigate the different or combined role of both the reinforcing particles and the process parameters on the fracture paths.

EXPERIMENTAL PROCEDURE

Dissimilar joints of AA2024 and AA7075 aluminium alloys of 5 mm of thickness were produced via FSW process, through a CNC machine (VM-2, HAAS, Oxnard, CA) and employing a triangular H13 tool steel. Fig. 1a shows the CAD draws of the geometry and dimensions of the employed tool, while Fig. 1b depicts its real features. The chemical composition of the plates, listed in Tab. 1, was determined by Optical Emission Spectrometry (OES) (PMI Master Smart, Oxford Instruments, UK).

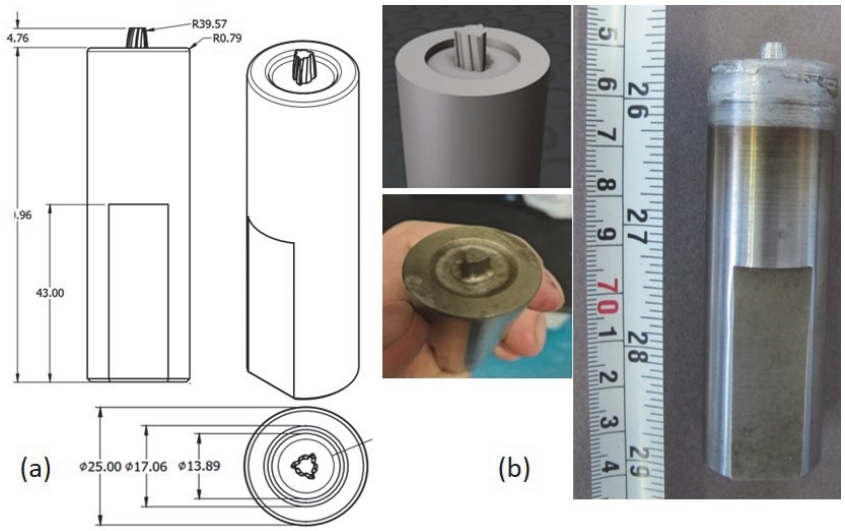

Figure 1: H13 FSW tool employed to produce the welds: a) CAD draws, b) real tool.

Material	Cu	Mg	Zn	Mn	Si	Fe	Al
AA2024-T351	4.80	1.62	0.047	0.653	0.0786	0.224	Bal.
AA7075-T651	1.59	2.85	5.82	0.0202	0.0696	0.189	Bal.

Table 1: Chemical composition (wt. %) of aluminium alloys.

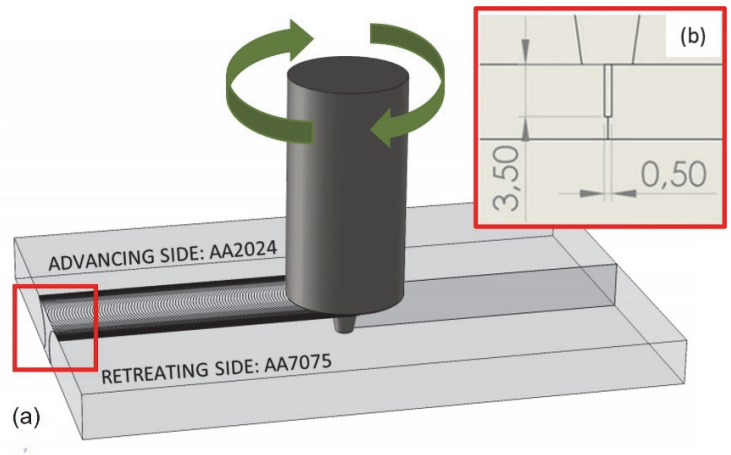

Figure 2: (a) Plates arrangement for joints production (b) Design of the groove machined on the adjoined sides of the plates (dimension in [mm]).

Given that the arrangement of the joint is of high importance in dissimilar joints, during the friction stir process AA2024 and AA7075 plates were placed on the advancing-retraining sides, respectively (see Fig. 2). This configuration was chosen considering that the process surely induces materials mixing and stirring, so significantly affecting the final microstructure

of the joint. Hence, to decrease the opposition of the material to flow, the metal with higher resistance was put on the retraining side while the one with lower resistance was arranged on the advancing side. This layout generally promotes a better mixing of both materials and, in turn, better quality joints [7]. Both un-reinforced and reinforced joints were performed; Al_2O_3 powder mixed with 2 wt.% SiC micropowder was employed as a reinforcement. In order to efficiently add the reinforcing particles into the joints the powder was preliminarily dissolved in alcohol and then added into the groove machined on the adjoined side of each plate.

The process parameters selected to produce the investigated joints were established using a full factorial 2^k design of experiments. Both rotational and translational speeds, together with the addition or not addition of the reinforcing particles, were considered as input parameters. Central and axial points proposed by Minitab® were used in order to have external values (low and high) for each factor. The full adopted parameters are summarized in Tab. 2; in particular, joints from FSW_1 to FSW_7 were fabricated without particles addition, while joints from FSW_8 to FSW_14 were produced by adding Al_2O_3-SiC particles.

The impact behaviour of the welds was evaluated by machining 10 mm × 5 mm × 55 mm unnotched Charpy impact specimens across the joints. Charpy impact tests were performed at room temperature (25 °C) by means of a CEAST Resil Impactor (Instron-CEAST, Pianezza, Italy) instrumented pendulum with 50 J of available energy. Three specimens for each condition were tested. Force-displacement data were recorded using a CEAST DAS 64K acquisition system and analysed using a tailored Matlab® code to remove noise and calculate the characteristic impact parameters according to the ISO 14556:2015 standard. The total energy was calculated as the integral of the force-displacement curve and the peak force F [kN] as the maximum load during the test. The energy absorbed at the peak force was calculated as initiation energy Ei [J], while the complementary energy from the peak force to the end of the test, estimated when the force reached the 2 % of its peak, was computed as propagation energy Ep [J]. Such parameters from each sample were correlated to the process parameters. Fig. 3a depicts the equipment employed to perform the impact tests as well as the arrangement from where they were obtained, Fig. 3b. Besides the impact behaviour, microstructural analyses were carried out by stereomicroscopy (SMZ 345T Infinity1, Nikon, Tokyo, Japan) on samples drawn from the joints for the detection of possible discontinuities and to measure the superficial area of wormhole defects identified across some welded joints. The microstructural features of the different characteristic zones of the FSWed joints as well as the reinforcing particles distribution were studied by optical microscopy (OM) (Eclipse MA20, Nikon) and by image analysis. Moreover, microstructural and fractographic analyses were also performed by Zeiss EVO MA 15 (Zeiss, Oberkochen, Germany) scanning electron microscopy (SEM) to investigate the combined role of the reinforcing particles and the process parameters on the propagation of fracture during Charpy tests and, in turn, their role in affecting the impact behaviour of the joint materials.

Joint	Microparticles addition	Rotational speed (rpm)	Translational speed (mm/min)
FSW_1		1000	54
FSW_2		1000	40
FSW_3		1000	40
FSW_4	No	1000	26
FSW_5		1000	40
FSW_6		1071	40
FSW_7		929	40
FSW_8		1050	50
FSW_9		950	50
FSW_10		1050	30
FSW_11	Yes	1000	40
FSW_12		1000	40
FSW_13		950	30
FSW_14		1000	40

Table 2: Designation of joints and corresponding process parameters according to the 2^k factorial design of experiments

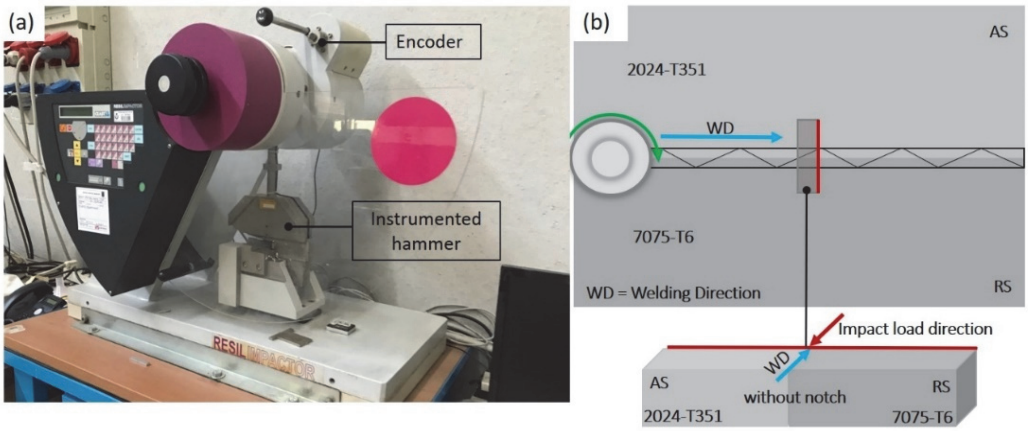

Figure 3: (a) CEAST Resil Impact instrumented pendulum and (b) machining position of the Charpy samples.

	Joint	Mean defect area (mm^2)
No	FSW_1	0.01 ± 0.02
	FSW_2	/
	FSW_3	/
	FSW_4	0.20 ± 0.02
	FSW_5	/
	FSW_6	/
	FSW_7	2.10 ± 0.03
Yes	FSW_8	2.86 ± 0.04
	FSW_9	0.77 ± 0.01
	FSW_10	2.33 ± 0.02
	FSW_11	1.42 ± 0.03
	FSW_12	1.02 ± 0.03
	FSW_13	1.49 ± 0.01
	FSW_14	1.26 ± 0.03

Table 3: Wormhole defect area analysis of the investigated joints.

RESULTS AND DISCUSSIONS

Macrostructural and microstructural analysis

Macrostructural analysis of joints produced with the addition of the reinforcing particles showed the presence of different discontinuities preferentially ascribed to wormhole defects and mainly localized at the bottom of the stir zones in most of the joints. In Tab. 3 the wormhole defects areas measured via image analysis in samples drawn from all the joints are reported; data are the mean values of the measurements performed on at least three samples

drawn from each joint. Despite the different employed process parameters, all the joints obtained with the addition of reinforcing particles showed the presence of wormhole defects in different sizes. Distribution and agglomeration of the reinforcing particles play a powerful role in the formation of these discontinuities, more crucial than the control of other process parameters. Joints obtained without any reinforcement, from FSW_1 to FSW_6, showed the almost absence of this kind of defect. Conversely, in joint FSW_7 the size of wormhole defects was found to be like most of the joints obtained with the addition of the reinforcing particles; macrostructural evidence of the joints' quality from FSW_1 to FSW_7 can be observed in Fig. 4. In Fig. 5 a comparison between two samples drawn from FSW_3 and FSW_8, respectively, is shown: sample FSW_3 presents the best quality among the ones drawn from un-reinforced joints, while sample FSW_8 obtained with the addition of particles and with the highest rotational and translational speeds exhibits the biggest wormhole defect. In accordance with different studies [14], [28], [29], the presence of a wormhole defect is due to a wrong managing of the process parameters, such as the rotational speed and advancing speed, since its bad control promotes an insufficient material flow and with this a lack of consolidation arousing the formation of the after-mentioned flaw.

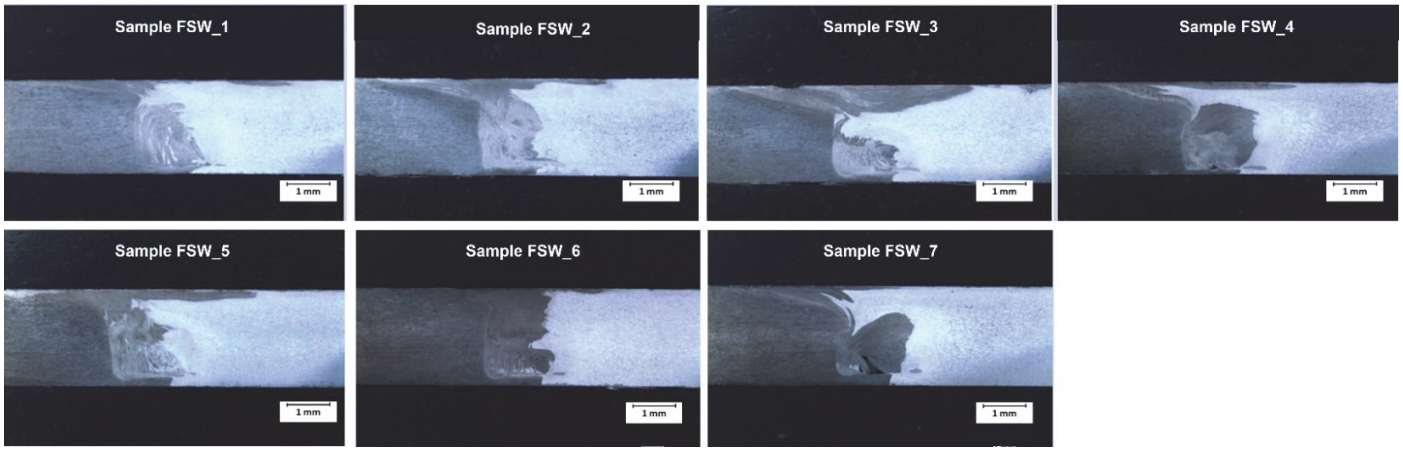

Figure 4: Macrographs of representative FSW_1 to FSW_7 samples.

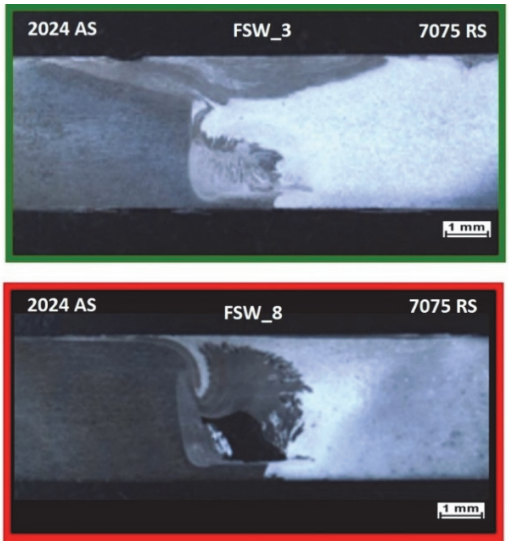

Figure 5: Macrographs comparing the joint quality between FSW_3 and FSW_8 samples.

Microstructural analyses performed by OM demonstrated the presence of the typical zones characterizing these solid-state joints, as well as the evolution of the microstructure across them. The onion ring shape on the stir zone (SZ), the flow of the metal in the thermo-mechanical zone (TMAZ) and at the interface between TMAZ and SZ, as well as the growing of

the microstructural features in the heat affected zone (HAZ), were clearly detected. In Fig. 6 the expected microstructural zones for representative samples of joints FSW_3 and FSW_11 is labelled and clearly identified.

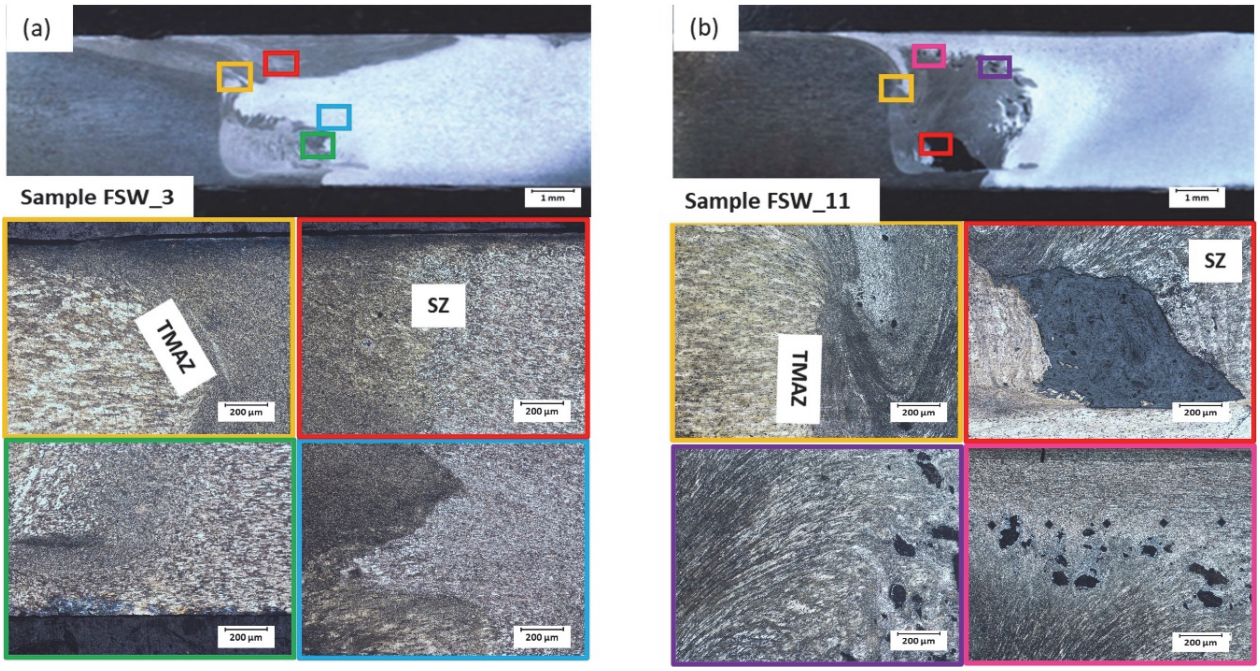

Figure 6: Typical microstructural zones of two FSWed samples: (a) FSW_3, (b) FSW_11

As mentioned before, it is well known that the distribution and agglomeration of the reinforcing particles play a very important role in the formation of discontinuities in FSWed joints. In Fig. 7 some details at high magnification of a sample drawn from joint FSW_11 have been highlighted: the blow-up SEM micrograph clearly shows how reinforcing particles agglomerated in the SZ during the process. A non-optimized mixing of the particles can promote the formation of clusters in the SZ causing both; an inefficient distribution of the particles inside the two joining materials and inadequate consolidation of the stirred metal, thus facilitating the formation of the wormhole defect.

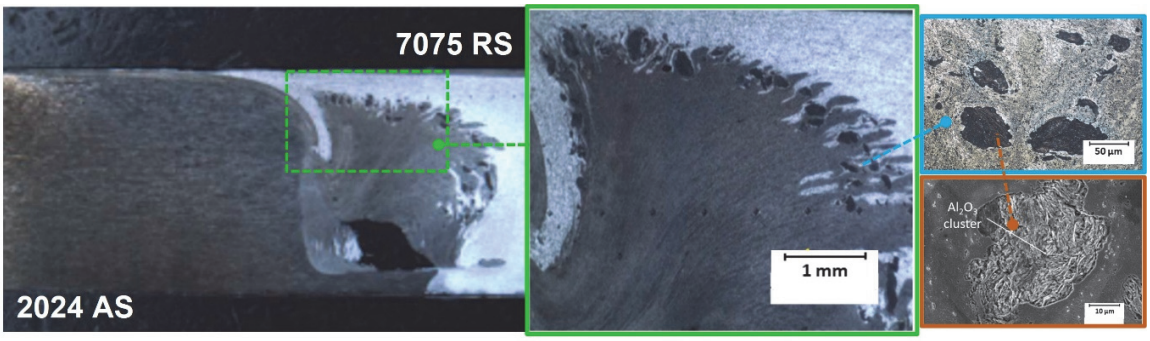

Figure 7: Details at high magnification of agglomeration of particles in sample FSW_11.

Impact properties

The average impact energies of the tested unnotched Charpy specimens are summarized in Fig. 8. According to the results and their low standard deviations, it is observed that specimens drawn from un-reinforced joints (FSW_1 to FSW_7) show higher total energies than the ones obtained with the addition of reinforcing particles (FSW_8 to FSW_14). This finding is clearly related to the presence of the wormhole defect, which significantly decreases the toughness of joints. Moreover, it can be observed that the impact energies of specimens drawn from un-reinforced joints are highly dependent on process parameters.

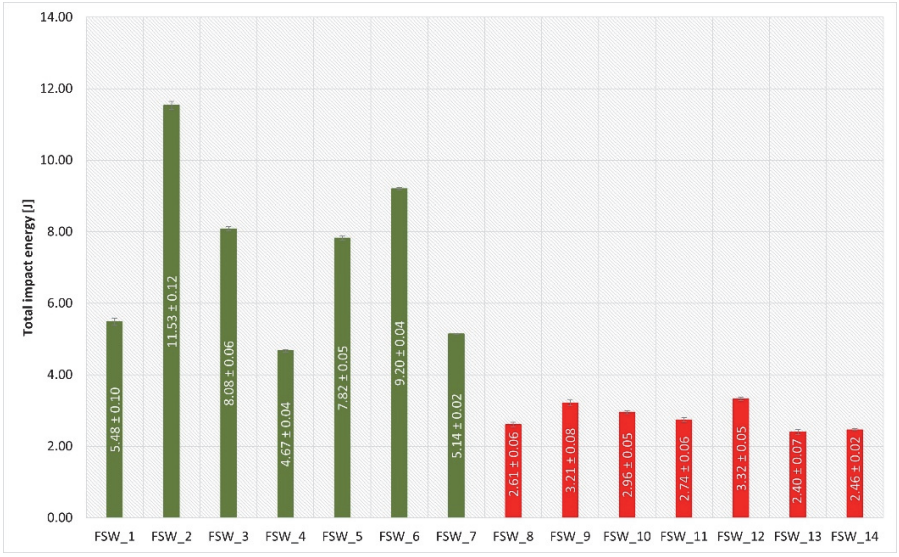

Figure 8: Total impact energies (green histograms refer to un-reinforced joints, red histograms refer to reinforced joints).

Fig. 9 shows the mean peak forces reached by the specimens during the tests. From these results it can be noticed that, as for total energies, joints FSW_1 to FSW_7 displays peak forces that are very sensitive to the process parameters. The highest values are observed for joints produced with 1000 rpm of rotational speed and 40 mm/s of translational speed. Conversely, for specimens with reinforcing particles, peak forces are quite independent from the combination of the process parameters; nevertheless, their peak values are lower than the ones characterizing the un-reinforced joints. Different authors ([30,31]) demonstrated that a homogeneous distribution of the reinforcing particles as well as their size and finesse are key factors to enhance the resistance of FSWed joints; hence, the agglomeration of reinforcing particles found in this investigation surely had a negative effect on the impact resistance of the joints. The formation of discontinuities, which negatively affect the impact properties, seems to be strictly correlated with the inhomogeneous distribution of the reinforcing particles.

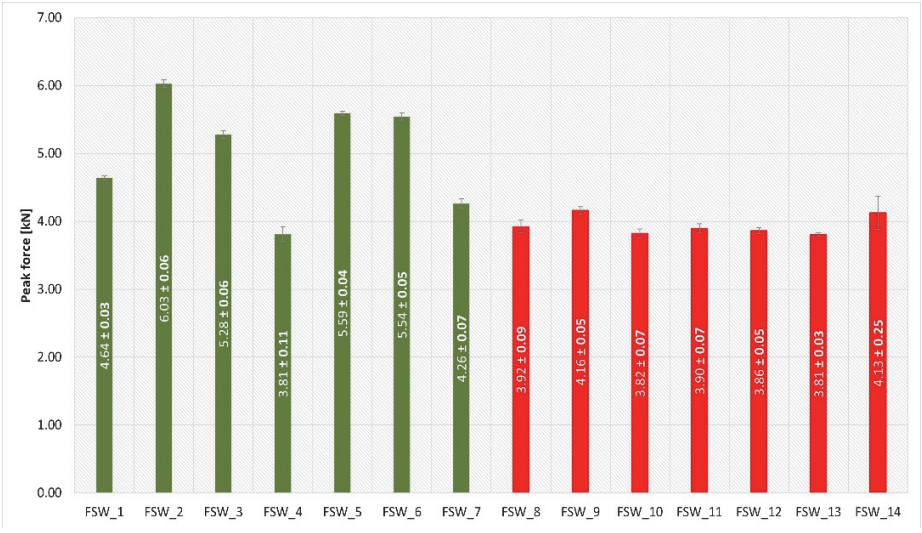

Figure 9: Peak forces (green histograms refer to un-reinforced joints, red histograms refer to reinforced joints).

Total absorbed energy was split into the two main complementary contributions, initiation energy (Ei) and propagation energy (Ep) and reported in Fig. 10 as a percentage of the total impact energy. In general, specimens drawn from joints produced without the addition of reinforcing particles show the highest contributions of Ei to the total energy, while reinforced joints display lower values of Ei % for most of the used process parameters. For two specific combinations of

rotational and translational speeds (FSW_10 and FSW_13) the two complementary contributions of the total energy are quite the same.

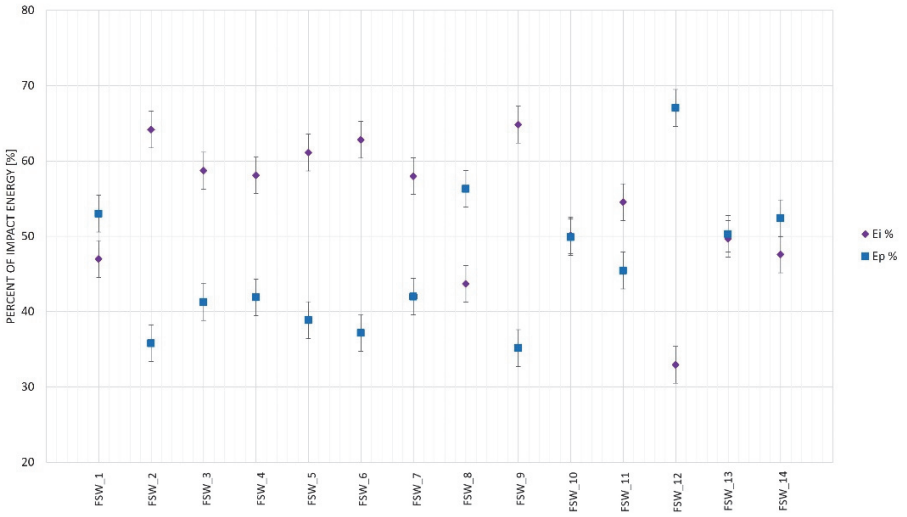

Figure 10: Percentage of absorbed energy during crack initiation (Ei %) and propagation (Ep %).

The force-displacement curves of the specimens which have absorbed the highest impact energies without and with the addition of reinforcing particles, respectively, are depicted in Fig. 11. These specimens, drawn from joints FSW_2 and FWS_12, were both produced with 1000 rpm and 40 mm/min. In sample FSW_2 the initiation energy and the peak force are significantly higher than in sample FSW_12. In sample FSW_2 the force drops down quite steeply after the peak force has been reached, while in sample FSW_12 after the initiation of the crack the material is initially able to resist its propagation dropping down just at the end of the test. Most of the specimens drawn from the reinforced joints show an increase of the contribution of Ep to the total energy, particularly the ones produced with a rotational speed higher than 950 rpm.

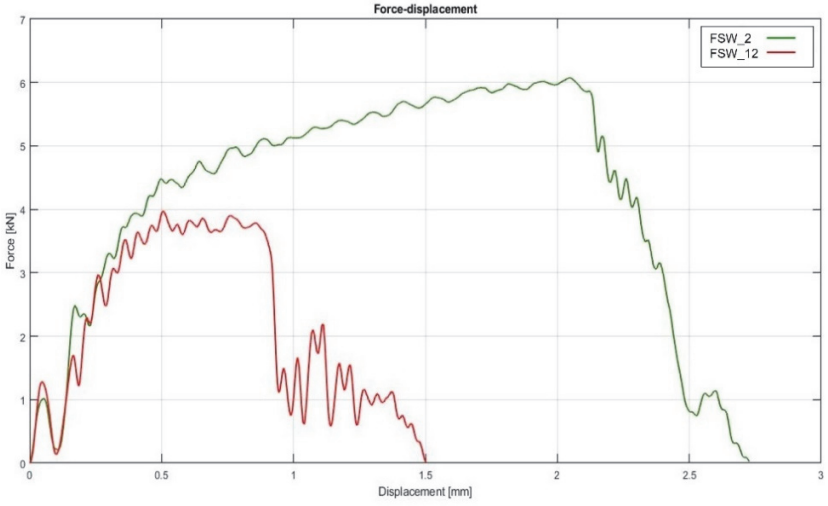

Figure 11: Force-displacement curves of two representative specimens drawn from FSW_2 and FSW_12 joints.

Fracture surface analysis

Fig. 12 and Fig. 13 show the most significant features of the fracture surface of specimens drawn from joints FSW_2 and FSW_12, whose impact behaviour was analysed in the previous paragraph. Firstly, at low magnification, it is possible to observe the macroscopic appearance of the fracture surfaces, that is the different zones interested by the propagation of

the crack during the impact strength test; in the blow-up SEM micrographs more details about the fracture mechanisms can be noticed. In specimen FSW_2 SZ and TMAZ are involved in the crack path and in both the presence of dimples can be ascribed to the formation of microvoids, which is the predominant fracture mechanism. In specimen FSW_12 are clearly visible different zones: in the top the typical SZ nugget, characterized by the presence of agglomerated reinforcing particles, in the middle the SZ with low density of reinforcing particles, and in the bottom the wormhole defect generated during the friction stir welding process. The presence of the wormhole defects along the crack path is mainly responsible for the lowest values of both the initiation energy and the peak force of reinforced specimens. The inhomogeneous distribution of the reinforcing particles also contributes to the peak force decreasing during the crack initiation. initiation of the crack.

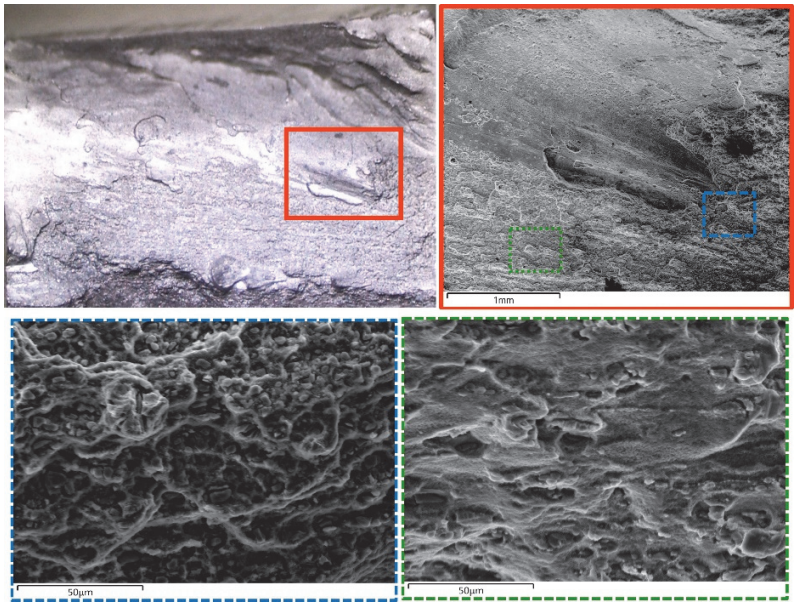

Figure 12: Fracture surface analysis of specimen FSW_2

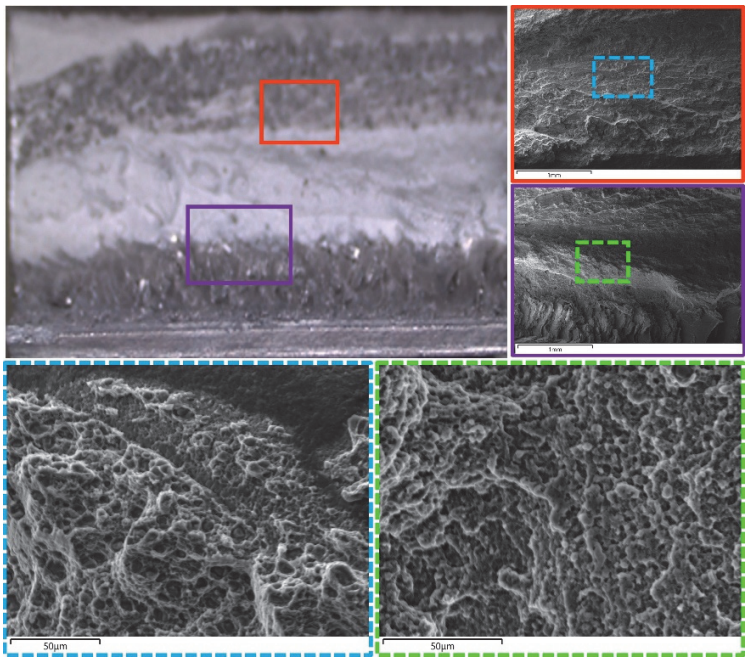

Figure 13: Fracture surface analysis of specimen FSW_12

CONCLUSIONS

Dissimilar AA2024-T351/7075-T651 FSWed joints, with and without the addition of Al_2O_3-SiC powder acting as a reinforcement, were developed using process parameters obtained from a 2^k design of experiments approach. Microstructural characterization was performed and correlated with the impact properties of unnotched Charpy impact samples machined from the joints. From the experimental findings, the following conclusions can be drawn:

- Welded joints obtained with the addition of reinforcing particles are prone to produce wormhole defects mainly related to insufficient material flow and to the unsound distribution of the reinforcement into the stir zone; agglomeration of particles was detected on the top of the stir zone in all the produced joints;
- Charpy specimens drawn from reinforced joints show lower impact absorbed energy and peak force than specimens machined from joints produced without the addition of reinforcing particles and their impact properties are less sensitive to process parameters. Although their lower impact properties, in reinforced specimens, the contribution of the propagation energy to the total energy is higher;
- According to the adopted 2^k design of experiments, a 1000 rpm rotational speed together with a 40 mm/s translational speed seem to be able to guarantee the best impact properties for the investigated dissimilar AA2024-T351/7075-T651 FSWed joints;
- The fracture surfaces analysis confirmed that the presence of the wormhole defects along the crack path, together with the inhomogeneous distribution of the reinforcing particles, is mainly responsible for the lowest impact properties of reinforced joints.

REFERENCES

[1] Debbarma, S., Sarkar, A., Saha, S.C. (2012). A Comparative Study on the Hardness Behaviour of Friction Stir Welding Aa6063 Lloy, J. Technol. Plast., 37(2), pp. 8.

[2] Mishra, R.S., Ma, Z.Y. (2005). Friction stir welding and processing, Mater. Sci. Eng. R Reports, 50, pp. 78, DOI: 10.1016/j.mser.2005.07.001.

[3] Alberti, N., Fratini, L. (2005). Friction stir welding: A solid state joining process, Adv. Manuf. Syst. Technol., pp. 20.

[4] Lohwasser, D., Chen, Z. (2010). Friction stir welding: From basics to applications, Florida, Woodhead Publishing Limited.

[5] Acerra, F., Buffa, G., Fratini, L., Troiano, G. (2010). On the FSW of AA2024-T4 and AA7075-T6 T-joints: An industrial case study, Int. J. Adv. Manuf. Technol., 48(9–12), pp. 1149–1157, DOI: 10.1007/s00170-009-2344-9.

[6] Bertrand, R., Robe, H., Texier, D., Zedan, Y., Feulvarch, E., Bocher, P. (2019). Analysis of AA2XXX/AA7XXX friction stir welds, J. Mater. Process. Technol., 271(March), pp. 312–324, DOI: 10.1016/j.jmatprotec.2019.03.027.

[7] Patel, V., Li, W., Wang, G., Wang, F., Vairis, A., Niu, P. (2019). Friction stir welding of dissimilar aluminum alloy combinations: State-of-the-art, Metals (Basel). 9(3), DOI: 10.3390/met9030270.

[8] Sen, M., Shankar, S., Chattopadhyaya, S. (2019). Investigations into FSW joints of dissimilar aluminum alloys, Mater. Today Proc., 27, pp. 2455–2462, DOI: 10.1016/j.matpr.2019.09.218.

[9] Acevedo, J.L., Morales, C.E., Rodriguez, B.R., Cerna, P.B. (2019). Microstructural and mechanical behavior study of 5052 aluminum alloy welded by FSW process, MRS Adv., 4(55), pp. 3041–3052, DOI: 10.1557/adv.2020.20.

[10] Salehi, M., Farnoush, H., Mohandesi, J.A. (2014). Fabrication and characterization of functionally graded Al-SiC nanocomposite by using a novel multistep friction stir processing, Mater. Des., 63, pp. 419–426, DOI: 10.1016/j.matdes.2014.06.013.

[11] Balaji, N., Balasubramanian, K., Rajesh, E.K. (2018). Effect of Boron Carbide on Properties of Aluminum 6063 Alloy Joined By Friction Stir Welding, Int. J. Tech. Innov. Mod. Eng. Sci. (IJTIMES), 4(02), pp. 80–85.

[12] Kumar, N., Patel, V.K. (2020). Effect of SiC/Si3N4 micro-reinforcement on mechanical and wear properties of friction stir welded AA6061-T6 aluminum alloy, SN Appl. Sci., 2(9), pp. 1–11, DOI: 10.1007/s42452-020-03381-y.

[13] Muhamad, M.R., Jamaludin, M.F., Yusof, F., Mahmoodian, R., Morisada, Y., Suga, T., Fujii, H. (2020). Effects of Al-Ni powder addition on dissimilar friction stir welding between AA7075-T6 and 304 L, Materwiss. Werksttech., 51(9), pp. 1274–1284, DOI: 10.1002/mawe.201900105.

[14] Vimalraj, C., Kah, P. (2021). Experimental review on friction stir welding of aluminium alloys with nanoparticles, Metals (Basel) 11(3), pp. 1–28, DOI: 10.3390/met11030390.

[15] Cubides-Herrera, C.S., Villalba-Rondón, D.A., Rodriguez-Baracaldo, R. (2019). Charpy impact toughness and transition temperature in ferrite–perlite steel, Sci. Tech., 24(2), pp. 205–211, DOI: 10.22517/23447214.19281.
[16] Raturi, M., Bhattacharya, A. (2021). Mechanical strength and corrosion behavior of dissimilar friction stir welded AA7075-AA2014 joints, Mater. Chem. Phys., 262(February), pp. 124338, DOI: 10.1016/j.matchemphys.2021.124338.
[17] Sirahbizu Yigezu, B., Mahapatra, M.M., Jha, P.K. (2013). Influence of Reinforcement Type on Microstructure, Hardness, and Tensile Properties of an Aluminum Alloy Metal Matrix Composite, J. Miner. Mater. Charact. Eng., 01(04), pp. 124–130, DOI: 10.4236/jmmce.2013.14022.
[18] Bahrami, M., Helmi, N., Dehghani, K., Givi, M.K.B. (2014). Exploring the effects of SiC reinforcement incorporation on mechanical properties of friction stir welded 7075 aluminum alloy: Fatigue life, impact energy, tensile strength, Mater. Sci. Eng. A, 595, pp. 173–178, DOI: 10.1016/j.msea.2013.11.068.
[19] Girelli, L., Giovagnoli, M., Tocci, M., Pola, A., Fortini, A., Merlin, M., La Vecchia, G.M. (2019). Evaluation of the impact behaviour of AlSi10Mg alloy produced using laser additive manufacturing, Mater. Sci. Eng. A, 748, pp. 38–51, DOI: 10.1016/j.msea.2019.01.078.
[20] Lattanzi, L., Merlin, M., Fortini, A., Morri, A., Garagnani, G.L. (2021). Effect of Thermal Exposure Simulating Vapor Deposition on the Impact Behavior of Additively Manufactured AlSi10Mg Alloy, J. Mater. Eng. Perform., 1059–9495, pp. 1–11, DOI: 10.1007/s11665-021-06414-8.
[21] Giovagnoli, M., Tocci, M., Fortini, A., Merlin, M., Ferroni, M., Migliori, A., Pola, A. (2021). Effect of different heat-treatment routes on the impact properties of an additively manufactured AlSi10Mg alloy, Mater. Sci. Eng. A, 802, pp. 140671, DOI: 10.1016/j.msea.2020.140671.
[22] Casari, D., Merlin, M., Garagnani, G.L. (2013). A comparative study on the effects of three commercial Ti-B-based grain refiners on the impact properties of A356 cast aluminium alloy, J. Mater. Sci., 48(12), pp. 4365–4677, DOI: 10.1007/s10853-013-7252-6.
[23] Devaiah, D., Kishore, K., Laxminarayana, P. (2016). Study the Process Parametric Influence on Impact Strength of Friction Stir Welding of Dissimilar Aluminum Alloys (AA5083 and AA6061) using Taguchi Technique, Int. Adv. Res. J. Sci. Eng. Technol., 3(10), pp. 15303–15310, DOI: 10.17148/IARJSET.2016.31018.
[24] Chen, T. (2009). Process parameters study on FSW joint of dissimilar metals for aluminum-steel, J. Mater. Sci., 44(10), pp. 2573–2580, DOI: 10.1007/s10853-009-3336-8.
[25] Zhang, C., Huang, G., Zhang, D., Sun, Z., Liu, Q. (2020). Microstructure and mechanical properties in dissimilar friction stir welded AA2024/7075 joints at high heat input: effect of post-weld heat treatment, J. Mater. Res. Technol., 9(6), pp. 14771–14782, DOI: 10.1016/j.jmrt.2020.10.053.
[26] Krishna, K.G., Devaraju, A., Manichandra, B. (2017). Study on Mechanical Propreties of Friction Stir Welded Dissimilar AA2024 and AA7075 Aluminum Alloy Joints, Int. J. Nanotechnol. Appl. ISSN, 11(3), pp. 285–291.
[27] Devaraju, A., Manichandra, B., Jeshrun Shalem, M., Manzoor Hussain, M. (2020). Impact on Mechanical properties & metallographic of solid state welded 2024 & 7075 Al alloys dissimilar joint by varying its parameters, Mater. Today Proc., 24, pp. 937–941, DOI: 10.1016/j.matpr.2020.04.405.
[28] Kah, P., Rajan, R., Martikainen, J., Suoranta, R. (2015). Investigation of weld defects in friction-stir welding and fusion welding of aluminium alloys, Int. J. Mech. Mater. Eng., 10(1), DOI: 10.1186/s40712-015-0053-8.
[29] Dialami, N., Cervera, M., Chiumenti, M. (2020). Defect formation and material flow in Friction Stir Welding, Eur. J. Mech. A/Solids, 80(November 2019), pp. 103912, DOI: 10.1016/j.euromechsol.2019.103912.
[30] Patel, V., Li, W., Liu, X., Wen, Q., Su, Y. (2019). Through-thickness microstructure and mechanical properties in stationary shoulder friction stir processed AA7075, Mater. Sci. Technol. (United Kingdom), 35(14), pp. 1762–1769, DOI: 10.1080/02670836.2019.1641459.
[31] Patel, V., Badheka, V., Li, W., Akkireddy, S. (2019). Hybrid friction stir processing with active cooling approach to enhance superplastic behavior of AA7075 aluminum alloy, Arch. Civ. Mech. Eng., 19(4), pp. 1368–1380, DOI: 10.1016/j.acme.2019.08.007.